

# Simulating Attochemistry: Which Dynamics Method to Use?

Thierry Tran, Anthony Ferté, and Morgane Vacher\*

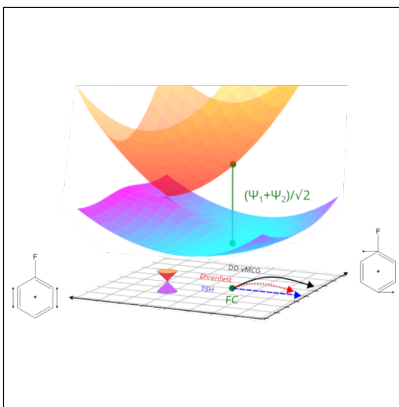
*Nantes Université, CNRS, CEISAM UMR 6230, F-44000 Nantes, France*

E-mail: [morgane.vacher@univ-nantes.fr](mailto:morgane.vacher@univ-nantes.fr)

## Abstract

Attochemistry aims to exploit the properties of coherent electronic wavepackets excited via attosecond pulses, to control the formation of photoproducts. Such molecular processes can in principle be simulated with various nonadiabatic dynamics methods, yet the impact of the approximations underlying the methods is rarely assessed. The performances of widely used mixed quantum-classical approaches, the Tully surface hopping, and classical Ehrenfest methods are evaluated against the high-accuracy DD-vMCG quantum dynamics. This comparison is conducted on the valence ionization of fluorobenzene. Analyzing the nuclear motion induced in the branching space of the nearby conical intersection, the results show that the mixed quantum-classical methods reproduce quantitatively the average motion of a quantum wavepacket when initiated on a single electronic state. However, they fail to properly capture the nuclear motion induced by an electronic wavepacket along the derivative coupling, the latter originating from the quantum electronic coherence property – key to attochemistry.

## TOC Graphic



In 2001, the first attosecond ( $10^{-18}$  s) domain pulses were generated.<sup>1-4</sup> Their application to polyatomic molecules sparked the emergence of the field known as “attochemistry”.<sup>5-9</sup> One distinctive characteristic of these ultrashort pulses is their broad energy bandwidth, capable of coherently exciting/ionizing to multiple electronic states of molecules.<sup>10-12</sup> Electronic wavepackets are non-stationary states: treating only the electronic degrees of the system, the electronic density of a wavepacket oscillates with a period inversely proportional to the energy difference between the populated electronic eigenstates.<sup>11</sup> In particular, due to interference effect, the electronic distribution of an electronic wavepacket is not the simple average of the individual electronic distributions of the different states. As a result, an electronic wavepacket can exhibit properties that markedly differ from those of pure states populated individually, potentially resulting in distinct chemical reactivity. One of the goals of attochemistry is to manipulate the outcome of photochemical reactions through the initial coherent excitation of electronic wavepackets with specific compositions.<sup>13,14</sup> This concept, also referred to as charge-directed dynamics in the literature, has been explored experimentally and computationally in small systems.<sup>15-20</sup> Using the simplest case of excitation to a coherent superposition of two electronic states, the ensuing nuclear dynamics manifest as two components: an intrastate component combining the two adiabatic gradients and an interstate component along the derivative coupling. Notably, the second contribution, which arises from electronic coherence, gives emergent properties to electronic wavepackets compared to traditional photochemistry.<sup>21</sup>

Theoretically, simulating photochemical reactions induced by electronic wavepackets implies propagating coherently nuclear wavefunctions initiated on multiple electronic states.<sup>11</sup> The most accurate family of methods to simulate such processes is fully quantum dynamics among which the Multi-Configuration Time-Dependent Hartree (MCTDH)<sup>22</sup> approach is commonly employed. However, the computational cost scales exponentially with the size of the system on top of requiring pre-fitted potential energy surfaces (PES). This limits the theoretical studies to small molecules/model systems,<sup>23-26</sup> or medium-size molecules in

reduced-dimensionality.<sup>20,27</sup> Simulations on model systems are suitable for the description of mostly rigid systems but hardly generalizable to photoreactions in polyatomic molecules involving, for instance, isomerization or dissociation. Additionally, a calculation on a system with reduced degrees of freedom may miss some relevant features and bias the predicted dynamics.<sup>28</sup> To overcome these bottlenecks, the alternative in attochemistry has been to perform simulations with frozen nuclei (thus unable to investigate charge-directed reactivity),<sup>11</sup> or treating all nuclear degrees of freedom with mixed quantum-classical methods.<sup>29–31</sup> A popular example of such methods is Tully surface hopping (TSH) where a swarm of independent trajectories is propagated on adiabatic PES and able to hop between them.<sup>32–34</sup> Another common method is the classical Ehrenfest<sup>35</sup> where a mean-field is employed to propagate the independent trajectories on single time-dependent PES corresponding to the superpositions of electronic eigenstates. While mixed quantum-classical approaches are computationally more affordable for larger molecules, they do not treat correctly the electronic coherence – a fundamental key component for attochemistry. To balance a comprehensive quantum treatment of the electrons and nuclei with reasonable computational cost, one can use an approach based on Gaussian wavepackets (GWP) such as the Direct Dynamics variational MultiConfigurational Gaussian (DD-vMCG)<sup>36</sup> method: in that method, both nuclei and electrons are treated quantum mechanically and the localized nature of the GWP requires the evaluation of the PES up to second order at the center of the basis functions only (local harmonic approximation), allowing an *on-the-fly* quantum simulation.

Recent works have evaluated the effect of the choice of the dynamics methods and algorithms on femtochemistry with initial excitation to a single electronic state with little observed difference (in the absence of quantum nuclear tunneling).<sup>37–39</sup> In the context of attochemistry with initial coherent excitation to a superposition of electronic states, mixed quantum-classical methods, like Ehrenfest and TSH, are commonly employed in the literature.<sup>29–31,40–42</sup> However, the impact of the approximations underlying such dynamics methods on simulations of attochemical reactions remains unknown. The goal of the present letter

is to compare the suitability of several dynamics methods for charge-directed reactivity: DD-vMCG, TSH, and Ehrenfest (see Figure 1 for a schematic representation). While these three methods do not constitute a comprehensive list of all ways to simulate non-adiabatic dynamics available and described in the literature, they cover a diverse range of possible approaches. In particular, we have focused on methods that are popular and regularly used within the field of attosecond chemistry; the overarching goal is to evaluate the accuracy of the different dynamics methods specifically within that context.

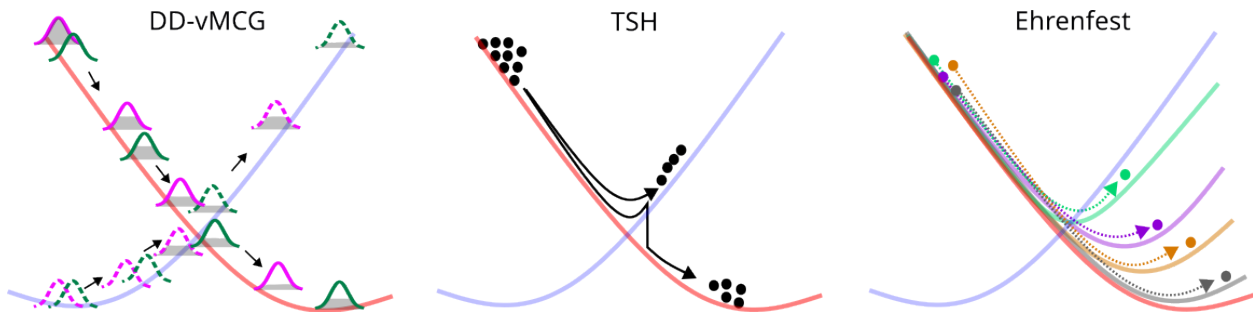


Figure 1: Scheme illustrating the three non-adiabatic dynamics methods employed in this work. (Left) DD-vMCG in the single-set formalism: a set of two interacting Gaussian wavepackets (pink and green) on each state (solid and dashed) are propagated in time and exchange population (grey filling). (Middle) TSH: a swarm of independent trajectories evolves in time following the slope of the “active” state curve and can jump from one state to the other. (Right) Ehrenfest: a swarm of independent trajectories evolving each on their individual time-dependent potential.

To assess the performances of the different dynamics methods, this letter focuses on the non-adiabatic dynamics upon photo-ionization of fluorobenzene. Attosecond pulses were initially exclusively and are still mainly in the XUV domain, thus leading to molecular ionization. Fluorobenzene is an ideal system for the investigation of coupled electron-nuclear dynamics as a conical intersection (CI) between the two lowest-energy cationic states is located in the vicinity of the neutral Franck-Condon (FC) point (see Figure 2). In general, the passage through a CI can lead to several photo-products, and the vicinity of an electronic states’ degeneracy upon ionization here allowed some of the present authors to test the control of nuclear motion near CI via electronic wavepackets.<sup>43</sup> The two lowest-energy states result from ionization from the  $\pi$  system: the  $D_0$  and  $D_1$  doublet adiabatic states have a so-called

*quinoid* and *anti-quinoid* diabatic characters, respectively, at the FC geometry. The states can also be labeled by their irreducible representation in the  $C_{2v}$  point group:  $B_1$  for the diabatic *quinoid* state ( $\Psi_Q$ ) and  $A_2$  for the diabatic *anti-quinoid* state ( $\Psi_A$ ). By mapping the PES in the two dimensions spanning the branching plane, derivative coupling ( $B_2$ ) and gradient difference ( $A_1$ ), the FC point is displaced from the lowest degeneracy point along the totally symmetric motion, i.e., gradient difference coordinate. At that geometry (see Figure 2), the gap between the two cationic states is about 0.27 eV.

The small size of the chosen system allows us to use a high-accuracy reference dynamics method, namely DD-vMCG, treating both electron and nuclear dynamics quantum mechanically, along with accurately capturing electronic coherence in full dimensions. The results for TSH and Ehrenfest methods shown here in the main manuscript are without decoherence correction and include the derivative coupling in the gradient for Ehrenfest and velocity rescaling along the nonadiabatic coupling direction for TSH. While it is standard to simulate photochemical reactions with an ad-hoc decoherence correction, we believe it may not be appropriate in the present context of attochemistry, where a superposition of electronic states is initially coherently populated. The electronic coefficients are propagated in time using explicit calculation of the nonadiabatic coupling vectors for both mixed quantum-classical methods. Results with alternative variants for TSH (for instance, with a decoherence correction) are shown in SI. In the present work, the focus is on the molecular dynamics induced by a coherent electronic superposition; we do not address the issue of creating the electronic wavepacket with a pulse, which has been covered from a theoretical point of view in the literature.<sup>12,44,45</sup> The dynamics are simulated for 10 fs and are started with two sets of initial electronic wavepackets: a set of pure electronic states either on the *quinoid* ( $\Psi_Q$ ) or *anti-quinoid* ( $\Psi_A$ ) state and a set of mixed superpositions of them with a 50-50 weight and either a positive or negative relative phase:  $\frac{1}{\sqrt{2}}(\Psi_Q + \Psi_A)$  and  $\frac{1}{\sqrt{2}}(\Psi_Q - \Psi_A)$ . It is noted that at the vertical ionization geometry, the chosen diabatic states are equal to the adiabatic ones. Also, we choose here to use the term “pure” when referring to a single adiabatic state, and

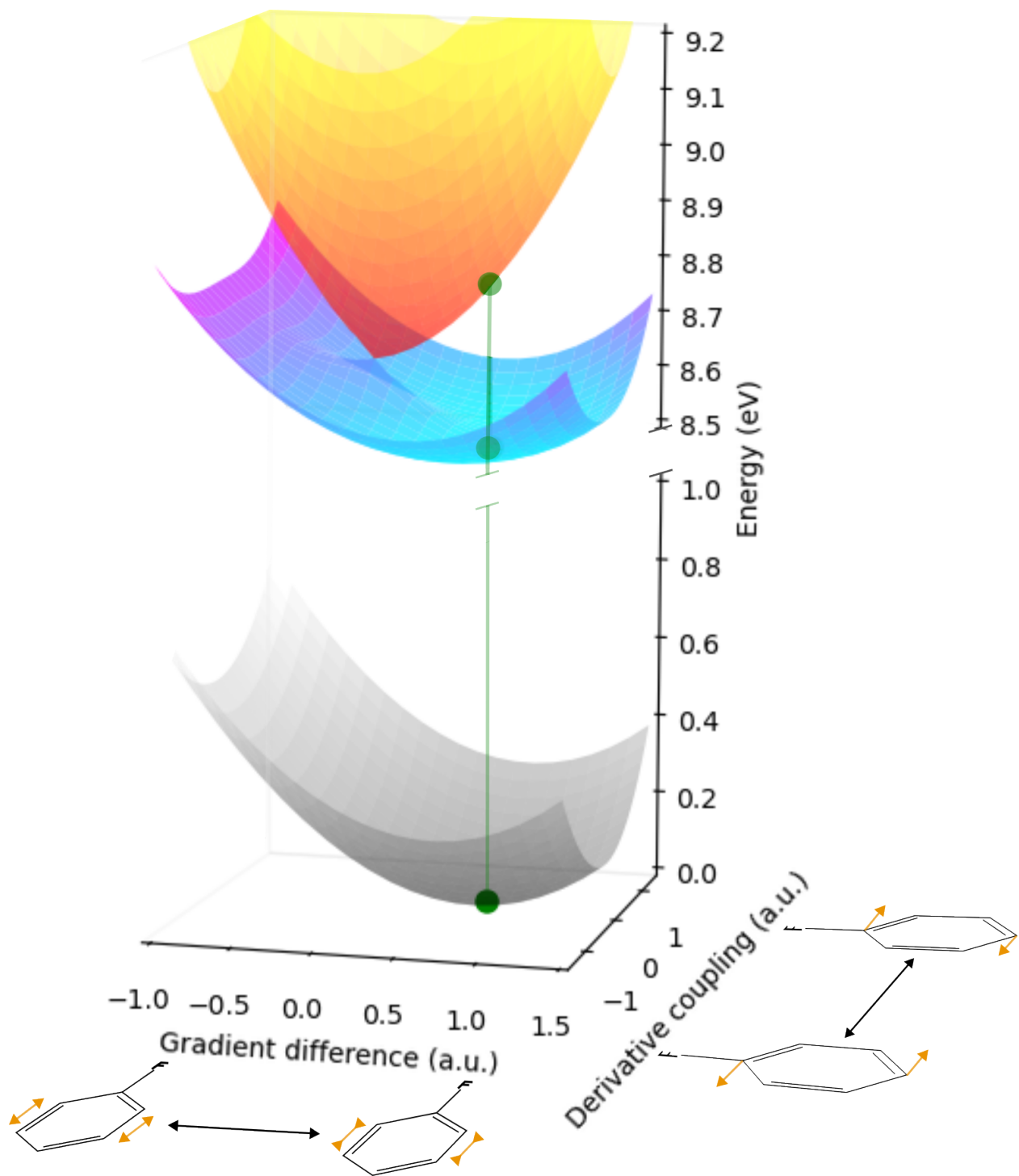


Figure 2: Adiabatic PES of the ground state of the neutral species (grey),  $D_0$  (blue-purple) and  $D_1$  (red-orange) cationic states along the gradient difference and derivative coupling coordinates with the main in-plane motion depicted on the molecule. The FC geometry is indicated by green dots.

“mixed” to a superposition of adiabatic states. Indeed, the adiabatic representation is natural when discussing charge migration and charge-directed reactivity in attochemistry, since these processes only occur when a coherent superposition of *adiabatic* states is populated.

In the following, we begin by presenting the set of pure state-induced dynamics, monitoring the average nuclear motion in the branching space spawned by the two lowest cationic states of fluorobenzene and the electronic population evolution. Afterward, we expand the analysis to dynamics initiated on coherent electronic superpositions and assess the accuracy of the mixed quantum-classical approaches for attochemical applications.

Figure 3a illustrates the average nuclear motion in the branching plane as predicted by the three methods, for the pure cases i.e., exciting to  $\Psi_Q$  (in blue) or  $\Psi_A$  (in red), akin to traditional photochemistry. By initiating the dynamics on an electronic eigenstate, due to symmetry, the center of the nuclear density only evolves along totally symmetric motion ( $A_1$  in  $C_{2v}$  point group) such as the gradient difference coordinate, until symmetry breaking is allowed by an event such as a passage through a CI. Here, consistently with the shape of the PES, dynamics initiated on the *anti-quinoid* state depicts an initial motion toward the CI along the gradient difference followed by a turning point, while the dynamics on the *quinoid* state move away from the CI. Both cases show negligible motion along the derivative coupling direction. The mixed quantum-classical methods qualitatively reproduce the reference DD-vMCG dynamics results. The main differences are the smaller amplitude of the motion along the gradient difference for the former and the displacement along the derivative coupling at the turning point. In the case of TSH, a slight drift in the direction of the derivative coupling is observed (also across other variants of TSH dynamics, see Figure S4 in SI). While one might initially attribute this drift to the hopping procedure, which rescales the velocity along the derivative coupling in the current procedure to conserve the total energy of the system, a similar trend is observed even when rescaling the full velocity vector. The use of the decoherence correction in TSH shows minimal to negligible impact on the nuclear dynamics within the 10 fs simulation range (see SI).

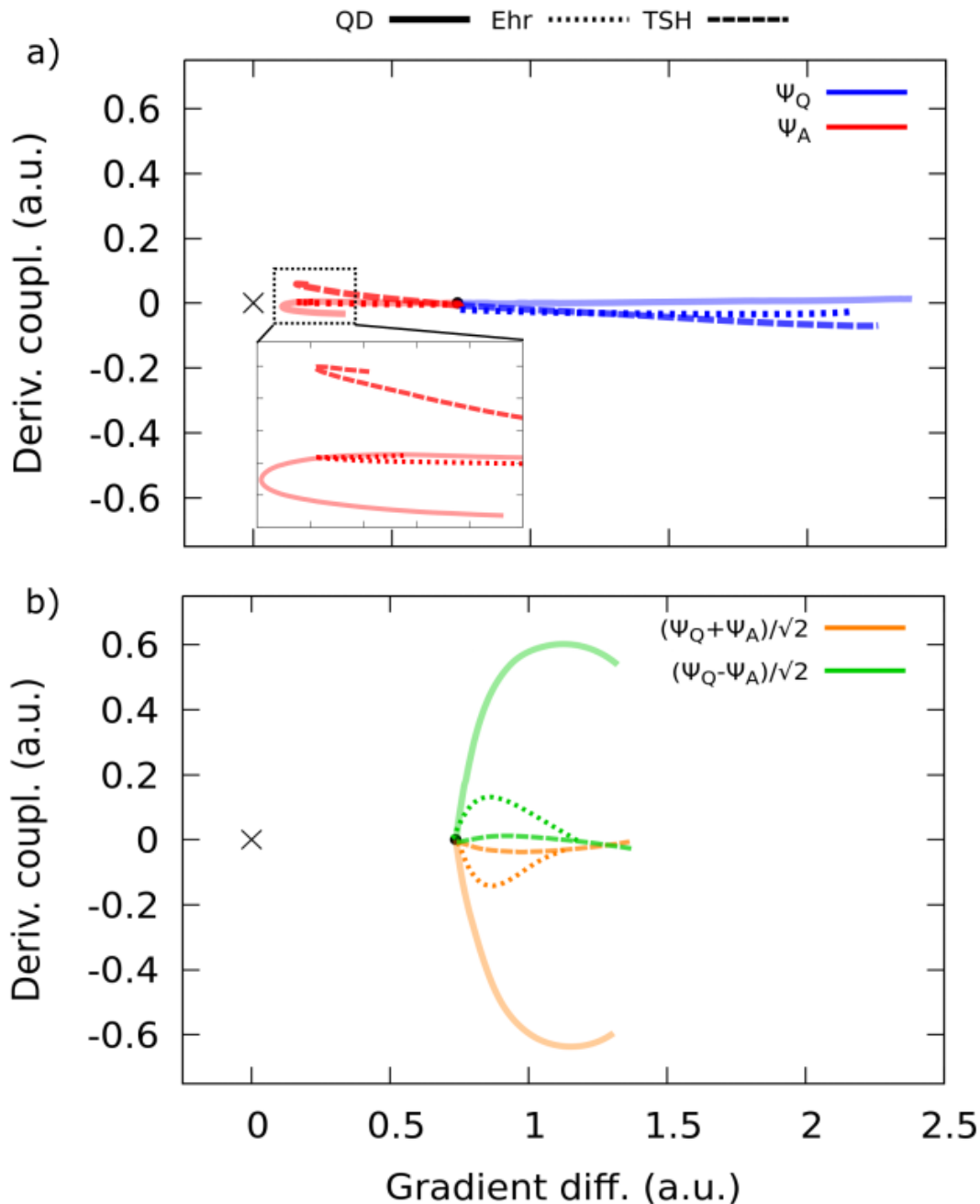


Figure 3: Nuclear motion averaged over all the GWP for DD-vMCG (solid) and trajectories for TSH (dashed) and Ehrenfest (dotted) methods in the branching space coordinates for a set of dynamics initiated (a) on a pure  $\Psi_Q$  (blue) or  $\Psi_A$  (red) state and (b) on a 50-50 mix of states i.e.,  $\frac{1}{\sqrt{2}}(\Psi_Q + \Psi_A)$  (orange) or  $\frac{1}{\sqrt{2}}(\Psi_Q - \Psi_A)$  (green) state. The CI (cross) is located at the origin and the FC point (dot) is at  $\sim 0.73$  along the gradient difference coordinate.

The associated adiabatic electronic population evolution is displayed in Figure 4a for the dynamics initiated on  $\Psi_A$  (see SI for  $\Psi_Q$ ). In DD-vMCG, the diabatic states are used for the

electronic representation, and as such, obtaining the adiabatic state population requires numerical integration as well as renormalization to avoid unphysical populations. The quantum dynamics display a rapid decay of the cationic excited state with the  $D_0$  state population dominating past 3.7 fs. The mixed quantum-classical dynamics display a slower decay to the ground state, with Ehrenfest being the slowest. It is noted that at the onset of the dynamics simulation, the adiabatic state populations are not exactly equivalent for the DD-vMCG wavefunction and classical trajectories; this is attributed to the initial geometries spread of the latter which is broader than the initial nuclear wavepackets of the quantum dynamics (see Figures S1 and S2 in SI).

Let us now shift our focus to the dynamics induced by mixed electronic wavepackets. Figure 3b shows the nuclear dynamics predicted by the three methods following excitation to a coherent superposition of the two lowest cationic states with two different relative phases, representative of an attochemistry experiment. With a coherent superposition of  $B_1$  and  $A_2$  states (*quinoid* and *anti-quinoid*, respectively), motion along the derivative coupling motion of irreducible character  $B_2$  becomes symmetry-allowed and the main driving force of the nuclear dynamics. Here, in the reference quantum dynamics (solid curve), a positive relative phase results in a distinct average motion in the negative direction of the derivative coupling, whereas the superposition with the negative relative phase yields a mirrored dynamics along the positive direction of the derivative coupling. This observation illustrates the concept of charge-directed reactivity sought in attochemistry, i.e., that the nuclear motion can be steered in a specific direction by controlling the composition and phase of the initial electronic wavepacket.

The quantum dynamics exhibits a turning point along the derivative coupling at approximately 0.6 a.u (Figure 3b), driven by two factors. Firstly, an adiabatic gradient develops from intrastate contribution, pointing toward the minimum. Secondly, the electron dynamics alters the relative phase between states, modifying the derivative coupling’s amplitude and direction. These effects gradually diminish the nuclear motion amplitude, potentially

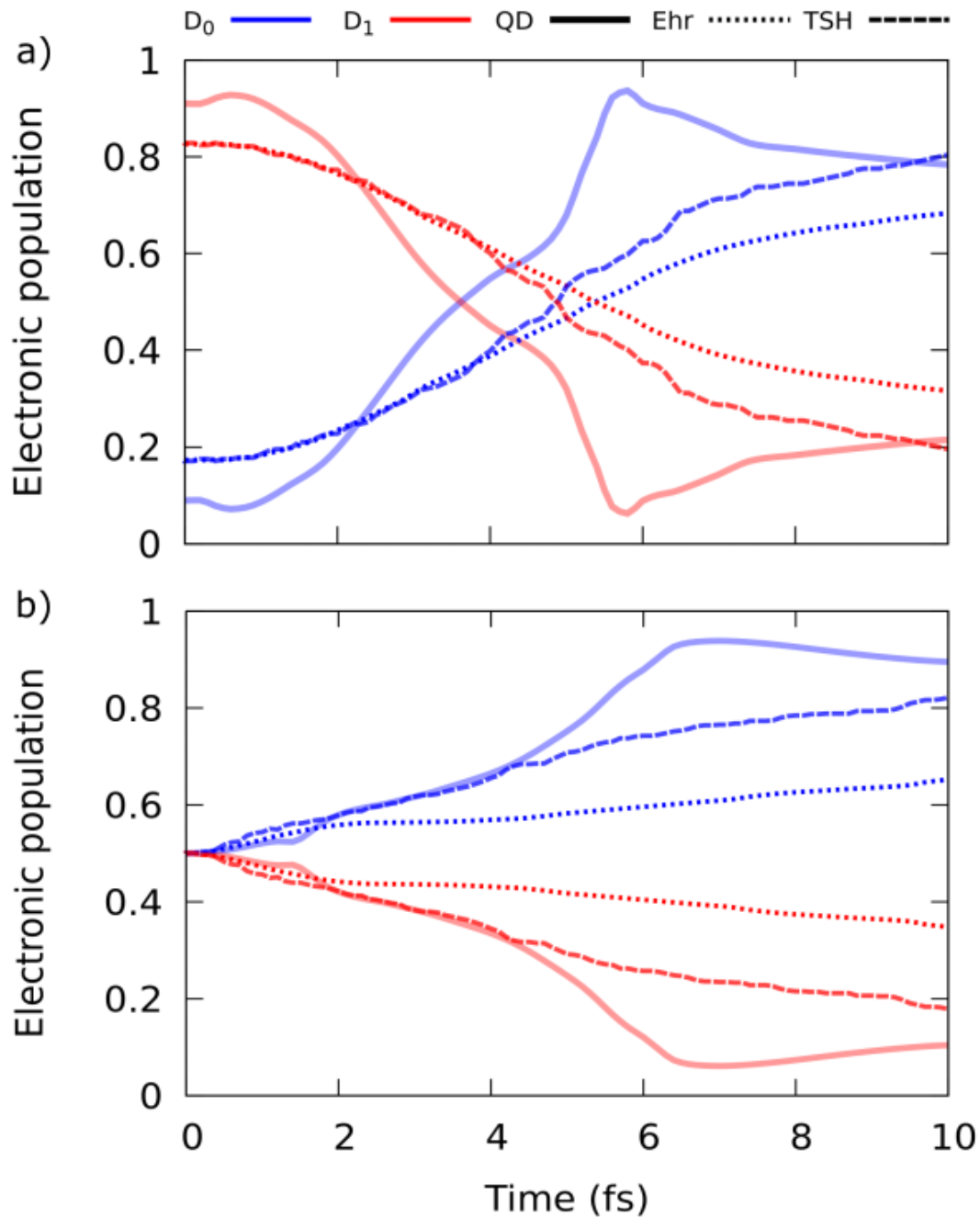


Figure 4: Adiabatic population averaged over all the GWP for DD-vMCG (solid) and trajectories for TSH (dashed) and Ehrenfest (dotted) methods as a function of time for a set of dynamics initiated on (a) the pure  $\Psi_A$  state and (b) the 50-50 mix with a positive relative phase  $\frac{1}{\sqrt{2}}(\Psi_Q + \Psi_A)$ .

reversing it along the derivative coupling coordinate. Both mixed electronic wavepackets lead to a motion in the positive direction of the gradient difference. This is attributed to  $\Psi_Q$

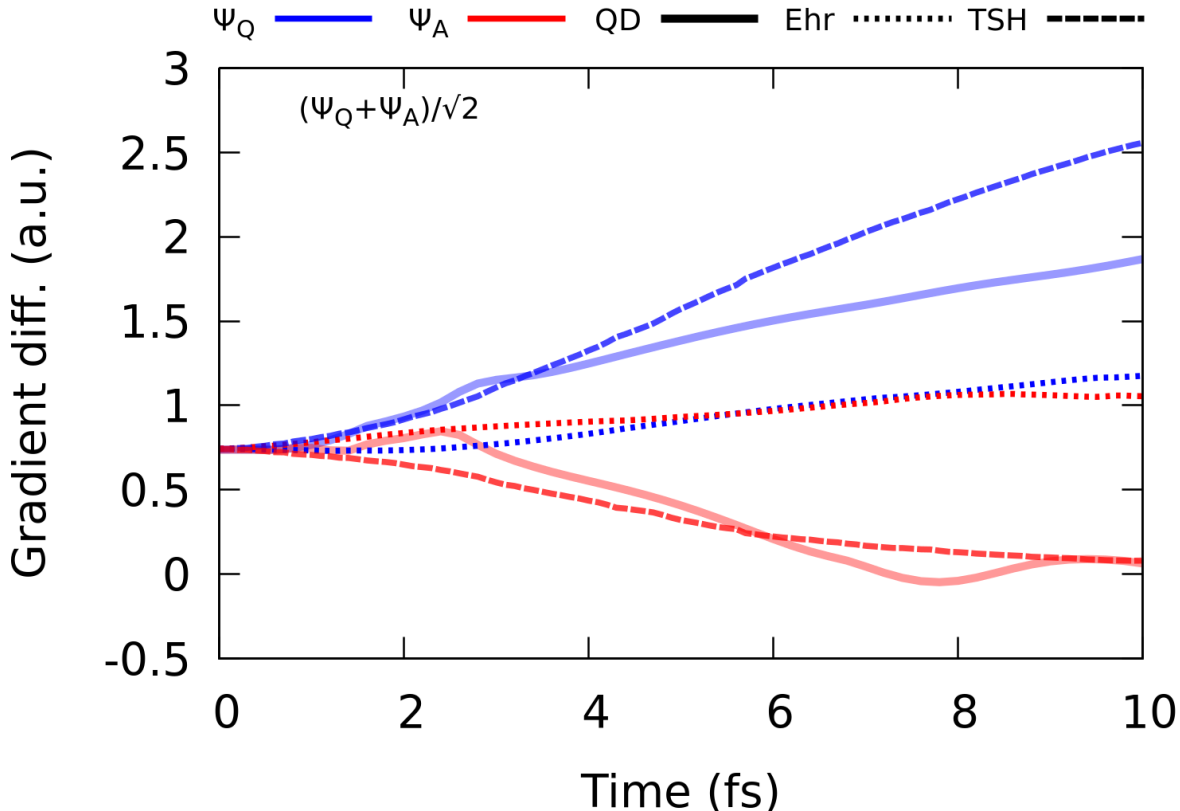


Figure 5: Nuclear motion averaged over all the GWP for DD-vMCG (solid line) and trajectories for TSH (dashed line) and Ehrenfest (dotted line) methods along the gradient difference over time for a set of dynamics induced by  $\frac{1}{\sqrt{2}}(\Psi_Q + \Psi_A)$ . The average corresponds to a weighted average based on the diabatic states for DD-vMCG and adiabatic states for TSH and Ehrenfest.

inducing larger motion than  $\Psi_A$  (Figure 3a), as well as the electronic wavepacket gradually de-exciting to the cationic ground state (Figure 4b). Additionally, Figure 5 depicts the average nuclear motion along the gradient difference vector over time induced by  $\frac{1}{\sqrt{2}}(\Psi_Q + \Psi_A)$  by projecting the nuclear wavepacket onto a specific electronic state. The diabatic states generate opposing forces along the gradient difference coordinate, hence a splitting of the nuclear wavepacket leading to decoherence.

We now present the attochemical dynamics predicted by the mixed quantum-classical methods. First, let us explain in more details the initial conditions used to simulate mixed electronic wavepackets. The trajectories are initiated with electronic amplitude coefficients corresponding to the coherent superposition of the two adiabatic states with either a positive

or negative relative phase. In addition, in TSH, the trajectories must be initiated on a specific so-called “active” state. The choice of an active state is natural when investigating photo-excitation/ionization to specific eigenstates, or multiple states but in an incoherent manner thus simulated individually. Here, for a given initial mixed electronic wavepacket, we have run two sets of TSH simulations, each with a specific adiabatic state as initially active. The TSH results presented here (dashed curve) are the average of the two dynamics sets. In general, TSH (dashed curve) and Ehrenfest (dotted curve) exhibit an average nuclear motion along the gradient difference that is similar to the quantum dynamics one (Figure 3b). However, both mixed quantum-classical methods predict qualitatively different nuclear motions along the derivative coupling (Figure 3b) and a slower non-adiabatic electronic decay to the  $D_0$  state (Figure 4) compared to reference results.

More precisely, the Ehrenfest dynamics show a distinct motion along the derivative coupling, consistent with the quantum dynamics, albeit with a smaller amplitude. In comparison, a single FC trajectory with no initial velocity displays a qualitatively similar motion in the branching space to a single GWP (see Figure S3 in SI). Thus, with similar initial conditions (geometry, velocity, and electronic wavepacket), the mixed quantum-classical mean-field approach yields comparable results to quantum dynamics for a single trajectory/GWP. However, the swarm of independent trajectories does not capture the proper quantum feature of the nuclear wavepacket: the classical trajectories on average show a faster return to the zero value along that coordinate. One driving component of charge-directed reactivity is the adiabatic state energy difference with a larger gap leading to faster electron dynamics, resulting in a quicker reversal of the gradient along the derivative coupling direction. Faster electron dynamics are expected for trajectories further away from the CI.

Additionally, the individual nuclear motions on different electronic states predicted by Ehrenfest qualitatively differ from the quantum dynamics results (Figure 5). It is important to note that the result shown in Figure 5 for mixed quantum-classical are a weighted average in the adiabatic basis (“active” state for TSH and adiabatic coefficients for Ehrenfest), and

thus not directly comparable to the DD-vMCG data in the diabatic basis. However, they provide a good qualitative picture of how the trajectories split based on the main driving electronic state. The Ehrenfest method is known to provide a long-time inaccurate nuclear density due to its inability to describe bifurcation of the wavepacket through CI and electronic decoherence.<sup>46–49</sup> This results here in a lack of splitting along the gradient difference as the trajectories maintain a high degree of mixing in the electronic wavepacket.

For TSH, the average nuclear motion induced by mixed electronic wavepackets displays very little to no displacement in the direction of the derivative coupling (Figure 3b, dashed curve). The TSH method is thus unable to properly capture the correct effect of the electronic coherence on the nuclear dynamics. Employing a different velocity rescaling method or decoherence correction yields very similar results (see Figure S4 in SI). Figure 5 shows a splitting of the nuclear wavepacket along the gradient difference. The motions are comparable to the reference data although the latter has a larger amplitude on the lowest cationic state. It is noted that the electronic population evolution induced upon excitation to mixed electronic wavepackets is similar to the one upon excitation to pure states (see Figure S6 in SI). This can be rationalized by how the electron dynamics, i.e., propagation of the equation-of-motions and hopping probabilities are evaluated: only the predicted change in population is relevant for hopping procedure in the Tully fewest switch algorithm.<sup>50</sup>

In summary, we have tested different dynamics methods to simulate attochemical processes, i.e., non-adiabatic dynamics induced by electronic wavepackets: DD-vMCG, Ehrenfest, and TSH. We have simulated the coupled electron-nuclear dynamics induced in fluorobenzene upon ionization and excitation to pure electronic states and coherent mixed electronic wavepackets, taking into account all nuclear dimensions. We have analyzed the nuclear motion in the branching space of the nearby CI to investigate the charge-directed reactivity. Mixed quantum-classical methods can reproduce quantitatively the quantum nuclear motion induced by pure electronic adiabatic states (or an incoherent superposition of them) as in standard photochemistry, consistently with literature.<sup>37–39</sup> In this case, the resulting

nuclear motion is mostly along the gradient difference coordinate, in the positive or negative direction depending on the excited electronic state.

On the other hand, the average nuclear motion induced by a mixed electronic wavepacket is characterized by an initial component mainly along the derivative coupling coordinate (with a splitting of the wavepackets on the different states along the gradient difference coordinate). This demonstration of charge-directed reactivity in a polyatomic molecule derives from electronic coherence. The most important conclusion of the present work is that none of the mixed quantum-classical methods tested here can capture the full quantum dynamics induced upon attochemical excitations, in particular the motion along the derivative coupling coordinate. This is due to the independent nature of the trajectories with initial conditions obtained from a phase space sampling, and propagating only on a single active state in the case of TSH. Moreover, the mean-field approach with Ehrenfest underestimates the adiabatic population transfer to the lowest cationic states and does not describe the splitting of the wavepackets along the gradient difference coordinate. Accurate simulation of attochemical dynamics induced by electronic wavepackets thus requires a full quantum treatment to describe properly the effect of electronic coherence on the subsequent nuclear dynamics and the resulting charge-directed reactivity. Further, it is interesting to note that the most accurate dynamics method predicts the strongest attochemical control of the nuclear motion. This was not obvious since mixed quantum-classical methods, suffering from overcoherence, could have overestimated the attochemical control. It is, therefore, a promising result for attochemistry.

## Methods

The reference results are obtained from a full quantum dynamics of fluorobenzene performed using Direct Dynamics variational Multi-Configurational Gaussian (DD-vMCG) implemented in the QUANTICS package<sup>51</sup> with the nuclei described by 10 Gaussian wavepack-

ets (GWP) evolving quantum mechanically and the electronic states are diabatised with the regularisation method. The mixed quantum-classical dynamics is done with the TSH and Ehrenfest methods using the SHARC program<sup>50</sup> for a set of 300 trajectories generated from a Wigner sampling. All electronic structure calculations are evaluated with the CASSCF(5e,6o) method with an active space containing the  $\pi/\pi^*$  orbitals with a 6-31G\* basis set. For DD-vMCG, the electronic structure is evaluated using the Gaussian program<sup>52</sup> and for SHARC dynamics, the OpenMolcas program<sup>53</sup> has been employed. In SHARC, in the absence of an external magnetic field, the doublet states are represented by a pair of degenerate states in either the molecular coulombic Hamiltonian or diagonal basis. Initializing the dynamics on either one or both degenerate states yield no difference in the present work. All simulations are done for 10 fs with a nuclear time step of 0.1 fs for TSH and Ehrenfest and adaptative time steps for DD-vMCG using the Runge-Kutta 5<sup>th</sup> order integrator.

## Acknowledgement

The project is partly funded by the European Union (ERC, 101040356 - ATTOP, M.V. and T.T.). Views and opinions expressed are however those of the author(s) only and do not necessarily reflect those of the European Union or the European Research Council Executive Agency. Neither the European Union nor the granting authority can be held responsible for them. We also thank the *Région des Pays de la Loire* who provided post-doctoral funding for A.F. The authors thank the CCIPL/Glicid mesocenter installed in Nantes and GENCI-IDRIS (Grant 2021-101353) for the generous allocation of computational time.

## Supporting Information Available

Trajectories initial conditions, analysis protocol, comparison of single Ehrenfest trajectory and GWP in branching space, results for variants of TSH (branching space and electronic adiabatic populations), trajectories densities along gradient difference and derivative cou-

plings as a function of time and convergence plots.

## References

- (1) Hentschel, M.; Kienberger, R.; Spielmann, C.; Reider, G. A.; Milosevic, N.; Brabec, T.; Corkum, P.; Heinzmann, U.; Drescher, M.; Krausz, F. Attosecond metrology. *Nature* **2001**, *414*, 509–513.
- (2) Paul, P. M.; Toma, E. S.; Breger, P.; Mullot, G.; Augé, F.; Balcou, P.; Muller, H. G.; Agostini, P. Observation of a Train of Attosecond Pulses from High Harmonic Generation. *Sci.* **2001**, *292*, 1689–1692.
- (3) Frank, F.; Arrell, C.; Witting, T.; Okell, A.; McKenna, J.; Robinson, J. S.; Hawthorth, C. A.; Austin, D.; Teng, H.; Walmsley, I. A. et al. Invited Review Article: Technology for Attosecond Science. *Rev. Sci. Instrum.* **2012**, *83*, 071101.
- (4) Duris, J.; Li, S.; Driver, T.; Champenois, E. G.; MacArthur, J. P.; Lutman, A. A.; Zhang, Z.; Rosenberger, P.; Aldrich, J. W.; Coffee, R. et al. Tunable isolated attosecond X-ray pulses with gigawatt peak power from a free-electron laser. *Nat. Photonics* **2020**, *14*, 30–36.
- (5) Remacle, F.; Levine, R. D. An electronic time scale in chemistry. *P. Natl. Acad. Sci. USA* **2006**, *103*, 6793–6798.
- (6) Calegari, F.; Ayuso, D.; Trabattoni, A.; Belshaw, L.; De Camillis, S.; Anumula, S.; Frassetto, F.; Poletto, L.; Palacios, A.; Decleva, P. et al. Ultrafast electron dynamics in phenylalanine initiated by attosecond pulses. *Sci.* **2014**, *346*, 336–339.
- (7) Kraus, P. M.; Mignolet, B.; Baykusheva, D.; Rupenyan, A.; Horný, L.; Penka, E. F.; Grassi, G.; Tolstikhin, O. I.; Schneider, J.; Jensen, F. et al. Measurement and laser control of attosecond charge migration in ionized iodoacetylene. *Sci.* **2015**, *350*, 790–795.

- (8) Barillot, T.; Alexander, O.; Cooper, B.; Driver, T.; Garratt, D.; Li, S.; Al Haddad, A.; Sanchez-Gonzalez, A.; Agåker, M.; Arrell, C. et al. Correlation-Driven Transient Hole Dynamics Resolved in Space and Time in the Isopropanol Molecule. *Phys. Rev. X* **2021**, *11*, 031048.
- (9) Månsson, E. P.; Latini, S.; Covito, F.; Wanie, V.; Galli, M.; Perfetto, E.; Stefanucci, G.; Hübener, H.; De Giovannini, U.; Castrovilli, M. C. et al. Real-time observation of a correlation-driven sub 3 fs charge migration in ionised adenine. *Commun. Chem.* **2021**, *4*, 73.
- (10) Breidbach, J.; Cederbaum, L. S. Universal Attosecond Response to the Removal of an Electron. *Phys. Rev. Lett.* **2005**, *94*, 033901.
- (11) Cederbaum, L.; Zobeley, J. Ultrafast charge migration by electron correlation. *Chem. Phys. Lett.* **1999**, *94*, 033901.
- (12) Nisoli, M.; Decleva, P.; Calegari, F.; Palacios, A.; Martín, F. Attosecond Electron Dynamics in Molecules. *Chem. Rev.* **2017**, *117*, 10760–10825.
- (13) Merritt, I. C. D.; Jacquemin, D.; Vacher, M. Attochemistry: Is Controlling Electrons the Future of Photochemistry? *J. Phys. Chem. Lett.* **2021**, *12*, 8404–8415.
- (14) Ferté, A.; Vacher, M. In *Chemical Modelling*; Bahmann, H., Tremblay, J. C., Eds.; RSC Publishing, 2022; Vol. 17; Chapter Recent advances in theoretical attosecond chemistry, pp 153–178.
- (15) Roudnev, V.; Esry, B. D.; Ben-Itzhak, I. Controlling  $\text{HD}^+$  and  $\text{H}_2^+$  Dissociation with the Carrier-Envelope Phase Difference of an Intense Ultrashort Laser Pulse. *Phys. Rev. Lett.* **2004**, *93*, 163601.
- (16) Kling, M. F.; Siedschlag, C.; Verhoef, A. J.; Khan, J. I.; Schultze, M.; Uphues, T.;

- Ni, Y.; Uiberacker, M.; Drescher, M.; Krausz, F. et al. Control of Electron Localization in Molecular Dissociation. *Sci.* **2006**, *312*, 246–248.
- (17) Kling, M. F.; Vrakking, M. J. J. Attosecond electron dynamics. *Annu. Rev. Phys. Chem.* **2008**, *59*, 463–492.
- (18) Rozgonyi, T.; González, L. Control of the photodissociation of CH<sub>2</sub>BrCl using a few-cycle IR driving laser pulse and a UV control pulse. *Chem. Phys. Lett.* **2008**, *459*, 39–43.
- (19) Lepine, F.; Ivanov, M. Y.; Vrakking, M. J. J. Attosecond molecular dynamics: fact or fiction? *Nat. Photonics* **2014**, *8*, 195–204.
- (20) Valentini, A.; van den Wildenberg, S.; Remacle, F. Selective bond formation triggered by short optical pulses: quantum dynamics of a four-center ring closure. *Phys. Chem. Chem. Phys.* **2020**, *22*, 22302–22313.
- (21) Tran, T.; Worth, G. A.; Robb, M. A. Control of nuclear dynamics in the benzene cation by electronic wavepacket composition. *Commun. Chem.* **2021**, *4*, 48.
- (22) Meyer, H.-D.; Manthe, U.; Cederbaum, L. The multi-configurational time-dependent Hartree approach. *Chem. Phys. Lett.* **1990**, *165*, 73 – 78.
- (23) Nikodem, A.; Levine, R. D.; Remacle, F. Spatial and temporal control of populations, branching ratios, and electronic coherences in LiH by a single one-cycle infrared pulse. *Phys. Rev. A* **2017**, *95*, 053404.
- (24) Despré, V.; Golubev, N. V.; Kuleff, A. I. Charge Migration in Propiolic Acid: A Full Quantum Dynamical Study. *Phys. Rev. Lett.* **2018**, *121*, 203002.
- (25) Schnappinger, T.; de Vivie-Riedle, R. Coupled nuclear and electron dynamics in the vicinity of a conical intersection. *J. Chem. Phys.* **2021**, *154*, 134306.

- (26) Dey, D.; Kuleff, A. I.; Worth, G. A. Quantum Interference Paves the Way for Long-Lived Electronic Coherences. *Phys. Rev. Lett.* **2022**, *129*, 173203.
- (27) Schüppel, F.; Schnappinger, T.; Bäuml, L.; de Vivie-Riedle, R. Waveform control of molecular dynamics close to a conical intersection. *J. Chem. Phys.* **2020**, *153*, 224307.
- (28) Gómez, S.; Heindl, M.; Szabadi, A.; González, L. From Surface Hopping to Quantum Dynamics and Back. Finding Essential Electronic and Nuclear Degrees of Freedom and Optimal Surface Hopping Parameters. *J. Phys. Chem. A* **2019**, *123*, 8321–8332.
- (29) Meisner, J.; Vacher, M.; Bearpark, M. J.; Robb, M. A. Geometric Rotation of the Nuclear Gradient at a Conical Intersection: Extension to Complex Rotation of Diabatic States. *J. Chem. Theory Comput.* **2015**, *11*, 3115–3122.
- (30) Vacher, M.; Mendive-Tapia, D.; Bearpark, M. J.; Robb, M. A. Electron dynamics upon ionization: Control of the timescale through chemical substitution and effect of nuclear motion. *J. Chem. Phys.* **2015**, *142*, 094105.
- (31) Vacher, M.; Albertani, F. E. A.; Jenkins, A. J.; Polyak, I.; Bearpark, M. J.; Robb, M. A. Electron and nuclear dynamics following ionisation of modified bismethylene-adamantane. *Faraday Discuss.* **2016**, *194*, 95–115.
- (32) Tully, J. C.; Preston, R. K. Trajectory Surface Hopping Approach to Nonadiabatic Molecular Collisions: The Reaction of  $H^+$  with  $D_2$ . *J. Chem. Phys.* **1971**, *55*, 562–572.
- (33) Tully, J. C. Molecular dynamics with electronic transitions. *J. Chem. Phys.* **1990**, *93*, 1061–1071.
- (34) Merritt, I. C. D.; Jacquemin, D.; Vacher, M. Nonadiabatic Coupling in Trajectory Surface Hopping: How Approximations Impact Excited-State Reaction Dynamics. *J. Chem. Theory Comput.* **2023**, *19*, 1827–1842.

- (35) Li, X.; Tully, J. C.; Schlegel, H. B.; Frisch, M. J. Ab initio Ehrenfest dynamics. *J. Chem. Phys.* **2005**, *123*, 084106.
- (36) Richings, G.; Polyak, I.; Spinlove, K.; Worth, G.; Burghardt, I.; Lasorne, B. Quantum dynamics simulations using Gaussian wavepackets: the vMCG method. *Int. Rev. Phys. Chem.* **2015**, *34*, 269–308.
- (37) Ibele, L. M.; Curchod, B. F. E. A molecular perspective on Tully models for nonadiabatic dynamics. *Phys. Chem. Chem. Phys.* **2020**, *22*, 15183–15196.
- (38) Janoš, J.; Slavíček, P. What Controls the Quality of Photodynamical Simulations? Electronic Structure Versus Nonadiabatic Algorithm. *J. Chem. Theory Comput.* **2023**, *19*, 8273–8284.
- (39) Gómez, S.; Spinlove, E.; Worth, G. Benchmarking non-adiabatic quantum dynamics using the molecular Tully models. *Phys. Chem. Chem. Phys.* **2024**, *26*, 1829–1844.
- (40) Trabatttoni, A.; Galli, M.; Lara-Astiaso, M.; Palacios, A.; Greenwood, J.; Tavernelli, I.; Decleva, P.; Nisoli, M.; Martín, F.; Calegari, F. Charge migration in photo-ionized aromatic amino acids. *Philosophical Transactions of the Royal Society A: Mathematical, Physical and Engineering Sciences* **2019**, *377*, 20170472.
- (41) Delgado, J.; Lara-Astiaso, M.; González-Vázquez, J.; Decleva, P.; Palacios, A.; Martín, F. Molecular fragmentation as a way to reveal early electron dynamics induced by attosecond pulses. *Faraday Discuss.* **2021**, *228*, 349–377.
- (42) Arnold, C.; Larivière-Loiselle, C.; Khalili, K.; Inhester, L.; Welsch, R.; Santra, R. Molecular electronic decoherence following attosecond photoionisation. *J. Phys. B: At. Mol. Opt.* **2020**, *53*, 164006.
- (43) Ferté, A.; Austin, D.; Johnson, A. S.; Malhado, J. P.; Marangos, J. P.; Vacher, M. 2023, DOI: 10.48550/ARXIV.2309.08269.

- (44) Mignolet, B.; Gijsbertsen, A.; Vrakking, M. J. J.; Levine, R. D.; Remacle, F. Stereocontrol of attosecond time-scale electron dynamics in ABCU using ultrafast laser pulses: a computational study. *Phys. Chem. Chem. Phys.* **2011**, *13*, 8331–8344.
- (45) Lara-Astiaso, M.; Palacios, A.; Decleva, P.; Tavernelli, I.; Martín, F. Role of electron-nuclear coupled dynamics on charge migration induced by attosecond pulses in glycine. *Chem. Phys. Lett.* **2017**, *683*, 357–364, Ahmed Zewail (1946-2016) Commemoration Issue of Chem. Phys. Lett.
- (46) Prezhdo, O. V. Mean field approximation for the stochastic Schrödinger equation. *J. Chem. Phys.* **1999**, *111*, 8366–8377.
- (47) Jasper, A. W.; Nangia, S.; Zhu, C.; Truhlar, D. G. Non-Born-Oppenheimer Molecular Dynamics. *Acc. Chem. Res.* **2006**, *39*, 101–108.
- (48) Akimov, A. V.; Long, R.; Prezhdo, O. V. Coherence penalty functional: A simple method for adding decoherence in Ehrenfest dynamics. *J. Chem. Phys.* **2014**, *140*, 194107.
- (49) Mannouch, J. R.; Richardson, J. O. A mapping approach to surface hopping. *J. Chem. Phys.* **2023**, *158*, 104111.
- (50) Mai, S.; Avagliano, D.; Heindl, M.; Marquetand, P.; Menger, M. F. S. J.; Oppel, M.; Plasser, F.; Polonius, S.; Ruckebauer, M.; Yinan Shu, et al. SHARC3.0: Surface Hopping Including Arbitrary Couplings – Program Package for Non-Adiabatic Dynamics. 2023.
- (51) Worth, G. Quantics: A general purpose package for Quantum molecular dynamics simulations. *Comput. Phys. Commun.* **2020**, *248*, 107040.
- (52) Frisch, M. J.; Trucks, G. W.; Schlegel, H. B.; Scuseria, G. E.; Robb, M. A.; Cheese-

man, J. R.; Scalmani, G.; Barone, V.; Petersson, G. A.; Nakatsuji, H. et al. Gaussian 16 Revision C.01. 2016; Gaussian Inc. Wallingford CT.

- (53) Fdez. Galván, I.; Vacher, M.; Alavi, A.; Angeli, C.; Aquilante, F.; Autschbach, J.; Bao, J. J.; Bokarev, S. I.; Bogdanov, N. A.; Carlson, R. K. et al. OpenMolcas: From Source Code to Insight. *J. Chem. Theory Comput.* **2019**, *15*, 5925–5964.